WELDING RESEARCH

SUPPLEMENT TO THE *WELDING JOURNAL*, APRIL 1987

Sponsored by the American Welding Society and the Welding Research Council

Predicting the Fatigue Resistance of Steel Weldments

Close agreement with the experimental results supports the local stress-strain modelling approach to fatigue prediction

BY R. A. TESTIN, J.-Y. YUNG, F. V. LAWRENCE, JR., AND R. C. RICE

ABSTRACT. Long life (10^7 cycles) fatigue strength results for stress-relieved and shot-blasted mild steel cruciform welds at four nominal mean stress levels are reported. These results are compared with analytical fatigue strength predictions made using a model developed by Lawrence, *et al.* (Refs. 1, 2). The analytical predictions, which were made without prior knowledge of the experimental results, fell within 6% of the experimental values for all mean stress levels. The close agreement between the experimental results and the analytical predictions supports the general applicability of the local stress-strain approach for modelling the fatigue of welds. Results of this study also suggest that performing a notch root set-up cycle analysis and considering both axial and bending (joint straightening) stress components are critical to obtaining accurate fatigue strength predictions for steel weldments.

R. A. TESTIN, J.-Y. YUNG, F. V. LAWRENCE, JR., and R. C. RICE are with the University of Illinois at Urbana-Champaign, Urbana, Ill.

Introduction

If it were possible, structural design engineers would conduct exhaustive full-scale fatigue tests on fatigue critical weld details before placing them in service. Since such tests are usually too lengthy and costly, designers need proven analytical models which can predict the fatigue resistance of a component at an early stage of the design process and which consider all of the important variables: material properties, processing effects, loading conditions and geometry (plate thickness, weld size, lack of penetration size, weld angles, etc.).

KEY WORDS
Steel Weld Fatigue
Cruciform Weld
Weld Fatigue Testing
Local Stress-Strain
Residual Stress
Mean Stress
Shot Blasting
Stress Relief
Crack Initiation
Fatigue Predictions

The fatigue life of a weldment consists of a crack initiation/early crack-growth stage (N_I) and a crack propagation stage (N_p). At long lives ($>10^6$ cycles), the crack initiation stage (N_I) appears to comprise the largest fraction of the total fatigue life (Ref. 1). The four important factors which most influence the crack initiation life (N_I) are: applied stresses (both axial and bending components), stress concentration effects inherent to the geometry and loading condition on the joint, the notch root residual stresses which result from fabrication and processing, and the properties of the notch root material in which crack initiation takes place.

The purpose of this study was to generate constant amplitude, long-life (10^7 cycles) fatigue strength data for a given weld configuration at different mean stress levels, and to evaluate the accuracy of an analytical model in predicting the experimental results. The study focused on the long-life fatigue strength of stress-relieved and shot-blasted mild

Table 1—Chemistry and Mechanical Properties of Mild Steel Plate

Chemistry (wt-%)	C	Mn	S	P	Cr	Cu
	0.18	0.42	0.02	0.01	0.01	0.01

Mechanical Properties

	Longitudinal/ Transverse
Tensile strength (MPa)	390/385
Yield point (MPa)	259/250
Yield strength (0.2%, MPa)	241/239
Elongation in 51 mm (%)	36.8/33.2
Reduction in area (%)	66.4/60.8
Hardness (HB)	116

steel cruciform weld specimens.

Weld specimens were fabricated, stress relieved, shot blasted, saw cut, machined and strain-gauged at the Electro-Motive Division of General Motors. Fatigue tests were performed at Battelle Columbus Laboratories. Fatigue strength predictions were performed at the University of Illinois at Urbana-Champaign (UIUC) in conjunction with the Electro-Motive Division as a part of the UIUC Fracture Control Program. The analytical predictions were made without prior knowledge of the experimental results.

Experimental Program

Specimen Preparation

Cruciform weld specimens were fabricated from hot-rolled, plain carbon mild steel plate using the FCAW process with E70T-2 wire (450 A, 30 V, and 100% CO_2 shielding). The chemistry and mechanical properties of the steel are given in Table 1. The steel meets the chemical requirements for SAE 1017 and 1020 steel.

The dimensions of the weldment were chosen such that axial fatigue failures would occur at the weld toe—Fig. 1A. Guidance in choosing variables such as weld size (12.7 mm/0.5 in.) and lack of penetration (LOP) size (2.5 mm/0.10 in.) was obtained from the results of Ho and Lawrence (Ref. 2). There were some problems in this regard, in that tensile mean stress tests produced LOP initiation site failures. This problem was addressed by drilling out the LOP using a drill size just sufficient to remove the tips of the LOP. This procedure is discussed further in the following section.

Great care was taken to obtain the best possible joint alignment. Weldments were fabricated by fixturing 457-mm (18-in.) lengths and welding using a fully automatic process. Following fabrication, the 457-mm weldments were furnace stress relieved at 1150°F (2102°C) for 3 h. Following stress relief, the weldments were shot blasted. Each 457-mm weldment was then saw cut and machined to yield six or seven specimens. Weld start and stop areas were discarded. Approximately 105 specimens were prepared in this manner.

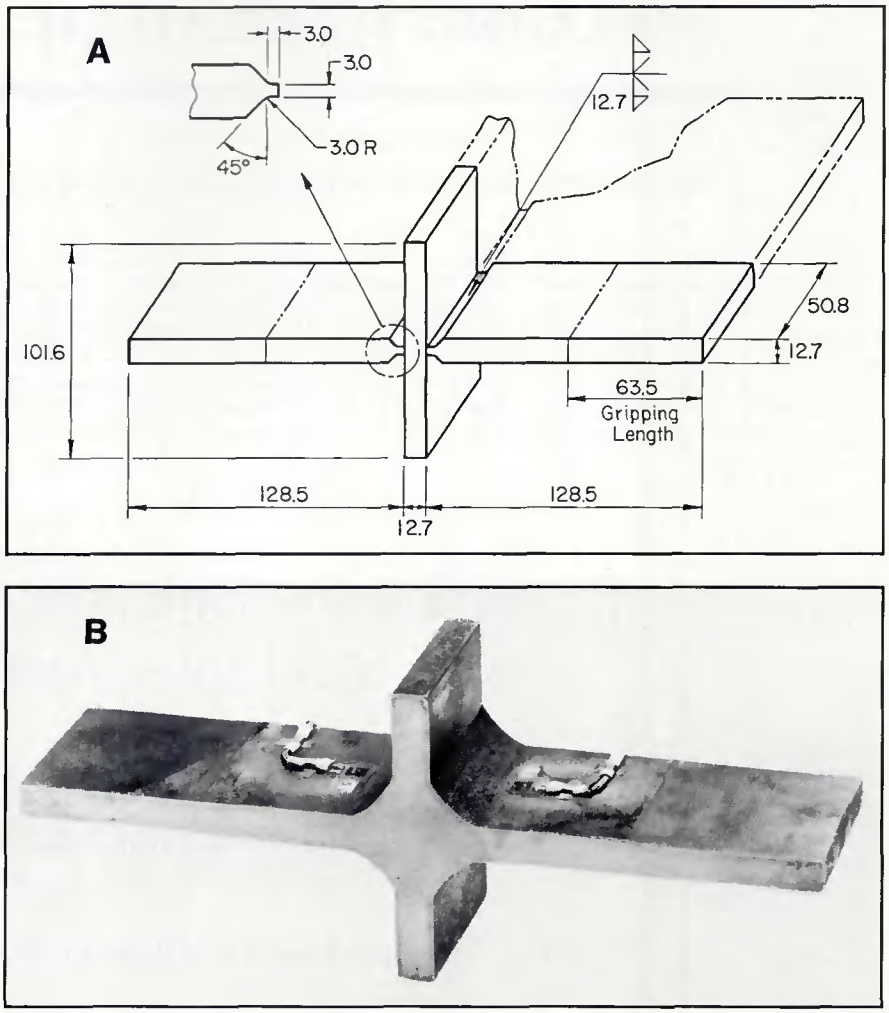

Fig. 1—A—Cruciform weld geometry (gripping surfaces are flat and parallel to each other within 0.025 mm for 63.5 mm); B—photograph of instrumented weld specimen

The residual stesses resulting from shot blasting were determined in several locations on two specimens using x-ray diffraction methods. Measurements on the plate surfaces (no attempt was made to measure residual stresses at the toe or in the weld metal) indicated that compressive residual stresses were approximately 217 MPa, or 90% of the yield strength of the mild steel plate. In our experience, this is typical of results for shot-peened mild steel.

Each specimen was instrumented with four 1.6-mm (0.06-in.) strain gauges located 5.6 mm (0.22 in.) from the weld toe on the centerline (both sides) of each load-carrying plate member. Gauge readings, which were considered in pairs, allowed partitioning of the axial and bending nominal stress components for each specimen. The 5.6-mm distance from the weld toe was selected based on recommendations of Ho and Lawrence (Ref. 2) that nominal stress conditions exist at a minimum distance of 0.3t (t = plate thickness) from the weld toe. The test specimen is shown in Fig. 1B.

The importance of machining the gripping surfaces of the specimens after shot blasting, as indicated in Fig. 1A, became evident during exploratory tests at the beginning of the program. Machining the gripping surfaces assured that the gripping surfaces were parallel and on the same centerline and eliminated initial bending stresses, which are usually introduced when specimens are clamped in test grips. Since the magnitude of both the mean and cyclic bending stresses can significantly affect axial fatigue test results, this procedure, which eliminated one of these extraneous variables, is recommended.

Test Program

All fatigue experiments were conducted in electro-hydraulic servo-controlled test systems. Two machines were utilized: one with 25 kip capacity and one

with 50 kip capacity. Large, 50,000-lb (22,727-kg) rated capacity hydraulic grips were used to clamp the specimens in the test machines. Grip alignment was verified through installation of a strain-gauged flat calibration bar; bending strains induced during tensile and compressive loading of this calibration bar were less than 0.2% of axial strains.

Four axial mean stress levels were selected for the investigation: +69 MPa (+10 ksi), zero, −34 MPa (−5 ksi) and −69 MPa (−10 ksi). Approximately 20 specimens per mean stress level were originally planned, but actual numbers tested at each mean stress level ranged from 13 to 27. The "staircase method" of testing was used initially to define test stress levels for subsequent use with the "two-point" method of determining median fatigue strength (Ref. 3). Only toe failures were considered in the fatigue strength analysis. Failures considered to be invalid included buckled specimens, failures at the gripping surfaces, and LOP failures.

As mentioned earlier, despite careful selection of specimen geometry parameters to favor weld toe failures, initial tests at the +10 ksi mean stress level produced only LOP failures. This problem was addressed and eliminated by drilling out the LOP, using a drill size just large enough to completely remove the LOP notch and leave a circular hole with a lower stress concentration factor. This action produced the desired weld toe failure location, and this procedure was followed for all +10 ksi mean stress level specimens. Finite element analyses of the drilled out LOP geometry and the original LOP geometry indicated that the elastic stress concentration factor at the weld toe was essentially identical for both conditions (within 1.4%). It was assumed that the hole drilling did not substantially alter the redistribution pattern of residual stresses.

Knowledge of the bending strains in the axial fatigue tests was vital to the analytical fatigue strength prediction portion of this study. Therefore, prior to each fatigue test, static strain surveys were performed on each specimen to measure the bending components of strain. Standard SR-4 type strain indicators were utilized to determine axial and bending strains at zero load, the intended maximum and minimum loads, and at several intermediate loads for each specimen. Specimens were then cycled at the selected mean and alternating axial stress levels with the test machines operating under load control.

Tests were conducted at room temperature in laboratory air. Test frequency was 30 Hz. Specimens were inspected frequently for crack initiation utilizing a "white grease" technique capable of detecting 0.76-mm (0.03-in.) surface length by 0.25-mm (0.01-in.) depth cracks at the weld toe. Detection of any crack(s) was considered specimen failure; otherwise, tests were carried out to 10^7 cycles before termination.

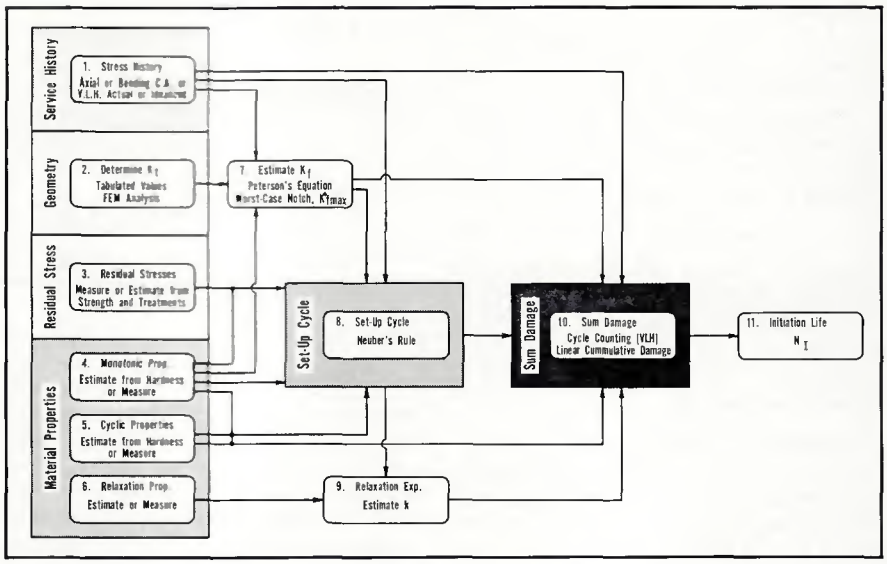

Fig. 2 — General scheme for estimating fatigue crack initiation life, N_I

Test Results

One hundred and three specimens were tested, of which 75 yielded valid results (Ref. 4). Median fatigue strengths as determined using the two-point method are reported in Table 2. Also included here are the average ratios of nominal bending stress to nominal axial stress determined for each mean stress level. These average ratios were used in the fatigue strength prediction calculations.

Estimating the Fatigue Life of Weldments

Estimating the Fatigue Crack Initiation Life, N_I

Lawrence, *et al.* (Refs. 1, 2), have developed a generalized model which predicts the fatigue strength of weldments. This model considers the total fatigue life (N_T) to be composed of a period devoted to crack initiation and early growth (N_I) and a period devoted to the growth of a dominant crack (N_p). While the total fatigue life is considered to be the sum of these two periods, at long lives, N_I dominates (Ref. 1) and the fatigue life or fatigue strength of a weld can be estimated by considering only crack initiation and early growth through the Basquin equation with the Morrow mean stress correction:

$$\Delta\sigma/2 = (\sigma'_f - \sigma_o)\,(2N_I)^b \qquad (1)$$

where $\Delta\sigma/2$ is the local (notch-root) stress amplitude at the crack initiation site, σ'_f is the fatigue strength coefficient for the material at the critical location, σ_o is the local mean stress determined after considering both residual and applied stresses (see next section, "Set-Up Cycle under Combined Loading"), $2N_I$ are the reversals devoted to crack initiation and early growth (one cycle equals two reversals), and b is the fatigue strength exponent.

The general scheme for estimating N_I is shown in Fig. 2 (Ref. 5). Each step in the analysis is numbered in the approximate sequence in which it is carried out. At the left are four categories of information which must be measured, collected and estimated (or guessed) to permit the calculation of the long-life fatigue strength or fatigue crack initiation life (N_I). One requires information about the service history, notch geometry, residual stresses, and notch-root materials properties. The accuracy of the predictions depends most heavily upon the level and nature of the applied stresses. The effects of geometry can be calculated with considerable accuracy using finite element methods. The appropriate values for residual stresses, σ_r, and particularly the material properties can usually be estimated without greatly diminishing the accuracy of the calculation. Having collected this information and used it to estimate the fatigue notch factor (K_f) and, if necessary, the stress relaxation constant (k), two main analyses, the set-up cycle analysis and the damage summation analysis, are then carried out.

The notch-root stress amplitude ($\Delta\sigma/2$) and mean stress (σ_o) which prevail during the fatigue life of a weld are established during the first few reversals of loading (set-up cycle). If no notch-root yielding occurs during this time, one can omit the set-up cycle analysis and assume elastic notch-root conditions. However, if notch-root yielding does occur during the first few applications of load, then a

set-up cycle analysis should be performed, and failure to do so could lead to incorrect estimates of the notch-root conditions during fatigue.

To relate local stress-strain conditions to the nominal stress-strain conditions, Neuber's rule, modified for fatigue by Topper (Ref. 6), is utilized:

$$\Delta\sigma\Delta\epsilon = (K\ \Delta S)^2/E \qquad (2)$$

where $\Delta\sigma$ and $\Delta\epsilon$ are the notch root stress and strain range, respectively, ΔS is the nominal stress range, and E is Young's modulus.

Worst Case Notch, K_{fmax}

The fatigue notch factor quantifies the severity of a discontinuity. Unfortunately, it is difficult to determine K_f for discontinuities such as a weld toe, because the notch root radii of such notches are generally unknown or difficult to measure and, what is worse, highly variable. To cope with the variable nature of the weld toe, Lawrence, *et al.* (Ref. 1), developed the concept of the "worst case notch," in which a radius giving the highest possible value of fatigue notch factor is presumed to occur somewhere at the weld toe or other similar notch. Experience with the notch size effect for steels had indicated that Peterson's equation correctly interrelates the fatigue notch and elastic stress concentration factors:

$$K_f = 1 + \frac{K_t - 1}{1 + \frac{a}{r}} \qquad (3)$$

where K_t is the elastic stress concentration factor (for a given notch geometry, notch-root radius, and nominal stress state), r is the notch-root radius (mm), and a is Peterson's material parameter, which may be approximated for steel by the expression $1.087 \times 10^5\, S_u^{-2}$ (mm), where S_u is the ultimate strength (MPa) of the notch-root material. A general form which can be used to describe the K_t of welds (Ref. 7) is:

$$K_t = \beta[1 + \alpha(t/r)^\lambda] \qquad (4)$$

where α, β and λ are constants whose values are determined by the weld geometry and the nature of the nominal stresses, and t and r are the plate thickness and notch-root radius, respectively. The worst case notch value of the fatigue notch factor, K_{fmax}, can be found by substituting Equation 4 into Equation 3 and differentiating with respect to r to determine the value of notch root radius for which the K_{fmax} condition exists. Since the constants β and λ are usually 1 and ½, respectively, K_t is often simply $1+\alpha(t/r)^{1/2}$, and it can be shown that K_{fmax} occurs at the notch-root radius numerically equal to Peterson's parameter a (*i.e.*, $r_c = a$) (Ref. 2).

The value of K_{fmax} depends upon the nature of the remote stresses (axial or bending) and the geometry of the joint through the constant (α), the ultimate strength of the material at the notch root (S_u), and the absolute size of the weldment through the dimension (t). Note that the use of the worst case notch concept leads to models which predict that the fatigue strength of a weldment depends upon its size as well as its shape, material properties and manner of loading.

$$K^A_{fmax} = 1 + 0.0015\ \alpha_A\ S_u t^{1/2} \qquad (5)$$

$$K^B_{fmax} = 1 + 0.0015\ \alpha_B\ S_u t^{1/2} \qquad (6)$$

where A and B represent the axial and bending loading conditions, respectively. Reference 7 lists K_t and K_{fmax} values for several weldments.

Set-Up Cycle Analysis under Combined Loading

Weldments are generally subjected to both axial and bending loads. The bending load often results from the straightening of weld distortions under load. When a weld is subjected to axial stresses, bending stresses, and residual stresses, the notch-root stress-strain response for the first application of load (that is, the first reversal {0-1}, as shown in Fig. 3) is limited by Neuber's rule, as modified for a combination of axial and bending stresses (Ref. 2).

$$\Delta\sigma\Delta\epsilon = (K^A_f\ S^A_1 + K^B_f\ S^B_1 + \sigma_r)^2/E \qquad (7)$$

where the superscript A is for the axial and the superscript B is for the bending loading conditions. The notch root stresses and strains at the end of the first reversal can be obtained by solving Equation 8 using the monotonic stress-strain properties (K, n) and the power law relation:

$$\Delta\epsilon = \Delta\sigma/E + z\left(\frac{\Delta\sigma}{zK}\right)^{1/n} \qquad (8)$$

where z equals 1 for initial loading and equals 2 for the subsequent simulation for materials which obey Massing's hypothesis (Ref. 8).

The notch-root stresses and strains at the end of the second {1-2} and subsequent reversals can be found in a similar manner using the cyclic stress-strain properties (K′, n′) and the expression:

$$\Delta\sigma\Delta\epsilon = (K^A_f\ \Delta S_A + K^B_f\ \Delta S_B)^2/E \qquad (9)$$

At the end of the first full cycle of the load history (two or three reversals), one can determine the notch-root stress amplitude ($\Delta\sigma/2$) and prevailing mean stress (σ_o). If the notch-root mean stress does not relax with continued cycling (*i.e.*, k is small), the fatigue crack initiation life can then be calculated using Equation 1.

Table 2—Test Results and Fatigue Strength Predictions

Nominal Axial Mean Stress (MPa)	Ratio of Nominal Bending Stress to Nominal Axial Stress	No. of Valid Tests	Fatigue Strength at $N_I = 10^7$ Cycles (MPa)		
			Predicted	Actual	Predicted/Actual
69	0.21	13	93	88	1.06
0	0.19	27	103	110	0.94
−34	0.15	15	109	116	0.94
−69	0.15	20	111	117	0.95

Fatigue Strength Predictions and Comparison with Experimental Results

The fatigue strength of the stress-relieved and shot-blasted cruciform weld specimens at four mean stress levels was estimated using the model discussed in the last section. The procedure followed the methodology diagrammed in Fig. 2 with one modification. Since it was desired to predict the (nominal) fatigue strength at a given life (not the life for a given stress condition), it was necessary to assume a value for nominal axial stress, use the experimentally determined ratio of bending to axial stress, and follow the methodology in Fig. 2, utilizing an iterative process until the desired life was obtained.

With reference to Fig. 2, the first step in the fatigue strength prediction procedure was to determine the ratio of nominal bending stresses to nominal axial stresses. This information, which was determined experimentally, was furnished and is given in Table 2. In Steps 2 and 7, values of K_t and K_{fmax} were calculated using the worst case notch concept and the ultimate tensile strength estimated in Step 4. The K_t values, calculated from equations in Ref. 2, were 4.56 and 2.98 for axial and bending stresses, respectively. These values correspond to K_{fmax} values of 2.78 and 1.99 for axial and bending stresses, respectively. These values were based on specimen dimensions in Fig. 1, assuming a 2.5-mm LOP and critical radius, r_c, of 0.14 mm ($r_c = a$).

Estimates of the required mechanical properties (Steps 4 through 6) were made from microhardness measurements in the region of crack initiation. Knoop microhardness measurements, taken at a depth of 0.25 mm (0.001 in.) from the weld toe,

Table 3—Estimated Mechanical Properties of Stress Relieved and Shot Blasted Weld Toe Material

Monotonic Property		
Ultimate strength (MPa)	S_u	793
Cyclic Properties		
Cyclic yield strength (MPa)	σ_y'	482
Fatigue strength exponent	b	−0.086
Fatigue ductility exponent	c	−0.60
Cyclic hardening exponent	n′	0.143
Cyclic strength coefficient (MPa)	K′	1172
Fatigue strength coefficient (MPa)	σ_f'	1124

were converted to Brinell hardness to estimate properties. The average weld toe material hardness was 160 HB after stress relief and 230 HB after shot blasting. Since it is difficult to estimate monotonic mechanical properties, other than tensile strength, from hardness, only the cyclic properties of the peened notch root material were used in the set-up cycle analysis. Table 3 lists the material properties used in Step 8; these were estimated using the hardness of the toe material and the relationships below:

Ultimate strength, MPa:

$$S_u = 6.9\ HB/2 \quad (10)$$

Cyclic yield strength, MPa (Ref. 9):

$$\sigma_y' = 0.608\ S_u \quad (11)$$

Fatigue strength exponent (Ref. 10):

$$b = -1/6 \log(2.1 + 917/S_u) \quad (12)$$

Fatigue ductility exponent:
c varies between −0.5 for hard steels and −0.7 for ductile steels

Cyclic strain hardening exponent (Ref. 11):

$$n' = b/c \quad (13)$$

Cyclic strength coefficient:

$$K' = \sigma_y' (0.002)^{1/n'} \quad (14)$$

Fatigue strength coefficient, MPa (Ref. 10):

$$\sigma_f' = 0.95\ S_u + 370 \quad (15)$$

In Step 3, the magnitude of the compressive residual stress at the shot blasted weld toe was assumed to be 50% of the ultimate strength of the stress relieved toe material (Ref. 12), *i.e.* −276 MPa (−40 ksi).

Set-up cycle analyses, Step 8, were carried out considering residual stresses, applied axial stresses, and bending stresses. Table 4 and Fig. 4 show the set-up

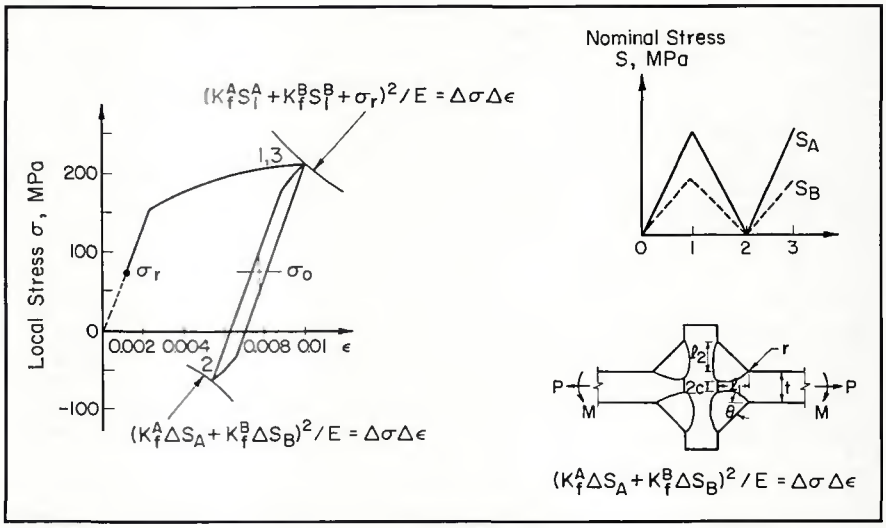

Fig. 3—Schematic illustration of a set-up cycle analysis

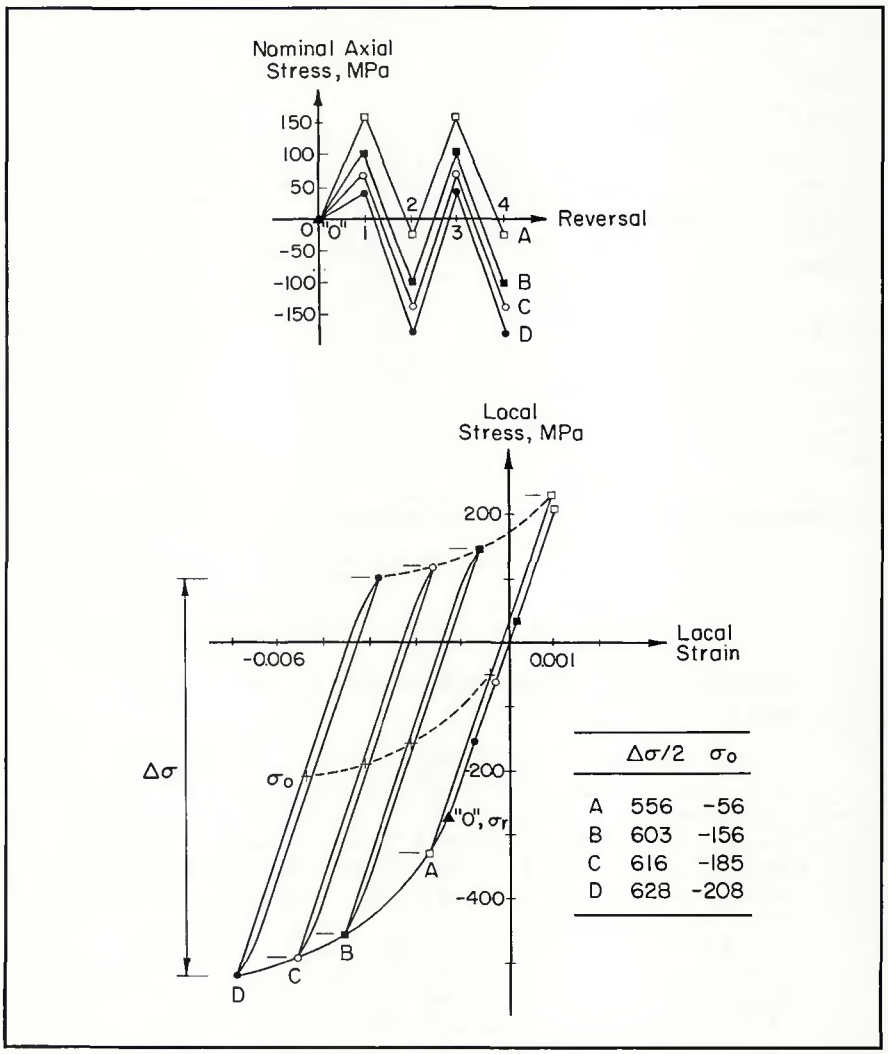

Fig. 4—Set-up cycle results for each mean stress level studied

Table 4—Set-up Cycle: Local Stress-Strain Estimates for Four Nominal Mean Stress Levels

Case	Measured Nominal Stresses (MPa) Axial	Bending	Estimated Local Stresses (MPa) (Strains)
A	0	0	−276 (−0.00133)
	162	34	214 (0.00104)
	−24	−5	−334 (−0.00177)
	162	34	223 (0.00101)
B	0	0	−276 (−0.00133)
	103	20	33 (0.00016)
	−103	−20	−458 (−0.00362)
	103	20	146 (−0.00055)
C	0	0	−276 (−0.00133)
	74	11	− 60 (−0.00029)
	−143	−21	−492 (−0.00471)
	74	11	123 (−0.00156)
D	0	0	−276 (−0.00133)
	42	6	−153 (−0.00074)
	−180	−27	−521 (−0.00597)
	42	6	106 (−0.00274)

cycle results for each mean stress level evaluated. Local mean stresses established in the set-up cycles were assumed not to relax because the mean stress relaxation exponents estimated in Steps 6 and 9 were very small.

Fatigue strength predictions at 10^7 cycles obtained by iteration of this process are compared to the actual test results in Table 2 and Fig. 5. Experimental results and predictions agreed within 6% in all cases.

Conclusions

Estimates of long-life fatigue strength obtained using a model developed by Lawrence, *et al.*, were within 6% of experimental results at the four mean stress levels investigated. The close agreement between the experimental results and the analytical predictions supports the general applicability of the local stress-strain approach for modelling the fatigue of welds. The results also suggest the importance of properly accounting for both axial and bending stress components and conducting a notch-root set-up cycle to estimate the prevailing notch-root stress conditions.

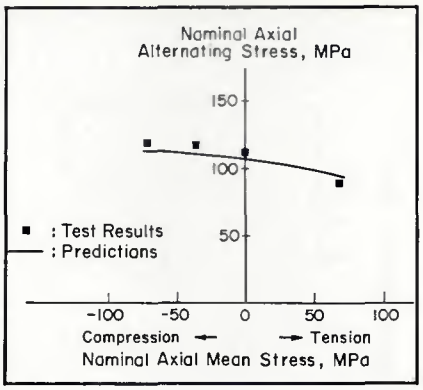

Fig. 5—Comparison of experimental results and fatigue strength predictions (10^7 cycles)

Acknowledgments

The authors are indebted to the Electro-Motive Division of General Motors Corporation for support of this work and for permission to publish the experimental results. The contributions of Dr. U. N. Nanda, Mr. J. F. Koch and Mr. J. D. Matyazic of the Electro-Motive Division in setting test program objectives and obtaining test specimens is gratefully acknowledged. The help of Mr. Omar L. Deel of Battelle Columbus Laboratories in overseeing the fatigue tests in this program is also acknowledged.

References

1. Lawrence, F. V., Jr., Mattos, R. J., Higashida, Y., and Burk, J. D. 1978. Estimation of fatigue initiation life of weld. ASTM STP 684, pp. 134–158.

2. Ho, N.-J., and Lawrence, F. V., Jr. 1984. Constant amplitude and variable load history fatigue test results and predictions for cruciform and lap welds. *Theoretical and Applied Fracture Mechanics* 1:3–21.

3. Little, R. E. 1975. *Manual on Statistical Planning and Analysis for Fatigue Experiments.* ASTM STP 588, pp. 54–60.

4. Rice, R. C., and Deel, O. L. 1985. Fatigue strength determination for cruciform-type welded steel specimens. Final Report from Battelle Columbus Laboratories to General Motors Corp.

5. Lawrence, F. V., Jr., and Yung, J.-Y. Estimating the effects of residual stress on the fatigue life of notched components. Accepted for publication in *Residual Stresses: Generation, Relaxation, Measurement, Prediction, Effects,* edited by Niku-Lari, A.

6. Topper, T. H., Wetzel, R. M., Morrow, JoDean. 1969. Neuber's rule applied to fatigue of notched specimens. *J. Mat.* 4:200–209.

7. Yung, J.-Y., and Lawrence, F. V., Jr. 1985. Analytical and graphical aids for the fatigue design of weldments. *Fatigue Fract. Eng. Mater. Struct.* 8:223–241.

8. Massing, G. 1926. Eigenspannungen und Verfestigung beim messing. *Proceedings of the 2nd International Congress of Applied Mechanics,* Zurich, Switzerland, p. 332.

9. Tanaka, K., Nishijima, S., Matsuoka, S., Abe, T., and Kouzu, F. 1981. Low- and high-cycle fatigue properties of various steels specified in JIS for machine structural use. *Fatigue Fract. Eng. Mater. Struct.* 4:97–108.

10. McMahon, J. C., and Lawrence, F. V., Jr. 1984. Predicting fatigue properties through hardness measurements. FCP Report No. 105, University of Illinois at Urbana-Champaign.

11. Morrow, JoDean. 1965. Internal friction, damping and cyclic plasticity. ASTM STP 378, pp. 45–87.

12. Chang, S. T., and Lawrence, F. V., Jr. 1983. Improvement of weld fatigue resistance. FCP Report No. 46, University of Illinois at Urbana-Champaign.